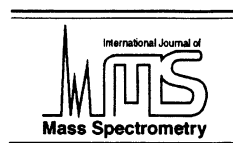




ELSEVIER



International Journal of Mass Spectrometry 177 (1998) 197–215

Photoionization investigation of cluster formation in heterocyclic compounds and their reactions with acidic species

Reiner P. Schmid^a, Johann-Georg Jäckel^a, Harold Jones^{a,*}, Gerhard Taubmann^b, Harutoshi Takeo^c

^aAbteilung Chemische Physik, and ^bAbteilung Theoretische Chemie, Universität Ulm, Albert Einstein-Allee 11, 89069 Ulm, Germany

^cNational Institute for Advanced Interdisciplinary Research, 1-1-4 Higashi, Tsukuba, Ibaraki 305, Japan

Received 23 March 1998; accepted 18 May 1998

Abstract

The formation of homogeneous molecular clusters by six different nitrogen-containing, heterocyclic (Het) compounds has been investigated using multiphoton ionization combined with time-of-flight mass spectrometry. The substances considered were pyridine, 3-picoline, 4-picoline, pyrazine, 2-methyl pyrazine, and pyridazine, and homogeneous clusters (Het)_n with $n \leq 15$ were observed. None of the clusters displayed sharp spectral features and consequently the information available was limited to mass spectra. In order to gain some information regarding the properties of these clusters, the effects of introducing the Lewis acids BF₃, BCl₃, and B(OH)₃ and also HF and HCl, into the free-jet expansion were investigated. The heterocyclic compounds listed above are all basic in character and consequently strongly bound complexes (donor–acceptor complexes) with these acids were expected to be formed. It was reasoned that a determination of the number of acidic molecules that attached themselves to a given cluster would give some insight into the structure of that cluster. The most extensive investigation was carried out with BF₃ and, surprisingly, not all the heterocyclics listed above formed mixed clusters with this Lewis acid under our experimental conditions. Our observations indicated the following: (1) the stability of the (Het)_n homogeneous clusters and the (Het)_n-(BF₃)_m mixed clusters appears to be related to the pK_a value associated with the heterocyclics involved; (2) under the conditions used in this work, the mixed clusters appear to be produced by the addition of BF₃ to homogeneous clusters that had already formed; and (3) the cations of mixed clusters in which $n = m$ are unstable and hence not detected. The results obtained with the other acids generally confirmed these conclusions and showed that the stability of the *cation* of the mixed cluster is the main factor influencing its detection. Ab initio calculations were also carried out and the results obtained are in good agreement with the experimental observations. These calculations showed there appears to be several structures for the pyridine dimer with similar stability. Several of these structures have two nonequivalent heterocyclic nitrogen atoms, which may explain the experimental observation that mixed-clusters containing only one BF₃ molecule appeared to be preferentially formed. (Int J Mass Spectrom 177 (1998) 197–215) © 1998 Elsevier Science B.V.

Keywords: Cluster formation and reaction; Photoionization; Heterocyclics

* Corresponding author.

1. Introduction

One of the often cited justifications for the investigation of the properties of Van der Waals complexes or molecular clusters is that this information is relevant to a basic understanding of the liquid phase. In order to make a meaningful contribution at this level, it is obviously necessary to produce data on increasingly large molecular clusters. However, in general, the quantity of detailed information obtainable on a particular cluster is usually inversely proportional to its size. For example, high resolution spectroscopic investigations have produced a wealth of very precise data on Van der Waals complexes containing two molecules or a molecule with a rare gas atom [1–6]. However, despite considerable recent technical advances, as the number of particles in the complex increases, the quality of the spectroscopic data obtained usually diminishes rapidly. Under favorable circumstances, the spectra may still yield good structural data on slightly larger clusters [7–9]. Although techniques, such as rotational coherence spectroscopy [10], which rely on high resolution in the time domain, will no doubt have many more contributions to make in the future, for larger clusters the situation will almost certainly remain difficult.

There are several reasons for the problems in obtaining structural information on molecular complexes from spectroscopic data as their size increases. Rotational resolution, which is the key to the determination of precise structure, very soon becomes impossible and, when dealing with electronic bands, only vibrational structure can be resolved. Even when the monomer displays sharp spectral features in its UV spectrum, with increasing clustering these may, deteriorating into broad, featureless regions of absorption.

It has been known for a number of years that heterocyclic compounds readily form clusters in a supersonic expansion [9,11,12]. With this type of molecule, the limit for carrying out rotationally resolved spectroscopy has already been exceeded with $n > 2$ and the spectra of higher clusters tend to be broad and featureless. As a result of this, there is very little information so far available on even small

homogeneous clusters (homoclusters) of this class of molecules. Because the pure liquids of all these substances presumably consist of such clusters, it would seem eminently desirable to gain experimental data on this type of aggregate.

The motivation for carrying out the work described in this article was to investigate a simple chemical approach to obtain structural information on clusters of heterocyclic compounds with n in the range of 2–15.

The basic idea, which served as a starting point for the experiments described in this article, is similar to that underlying the classical determination of structures via chemical reaction. It is well known that heterocyclic compounds form strongly bound donor–acceptor complexes with Lewis acids such as BF_3 . As is stated in many standard texts on inorganic chemistry, for example, the 1:1 complex of BF_3 with pyridine, (1:1 Py- BF_3 complex), is formed by the BF_3 molecule attaching itself to the lone electron pair of the nitrogen heteroatom of pyridine, forming a so-called donor–acceptor bond. The result is a solid substance with a boiling point of 300 °C and a binding energy of -46 kcal/mol [13] (i.e. roughly one third that of the average covalent bond).

This structure is supported by the results of photoelectron spectroscopy and ab initio calculations [14], which have shown that a configuration in which the boron atom of BF_3 is bound to the heteroatom is the most stable. Other structures in which BF_3 interacted with the π -system of the heterocyclic ring were considered theoretically [15] but were found to be energetically less favorable. A low resolution microwave investigation of the complexes of BF_3 with pyridine, pyrimidine, pyrazine, and pyridazine has also been carried out [16]. Although an effective rotational constant was obtained for a complex formed between a single BF_3 molecule and the first three heterocyclics named above, the amount of data obtained was too limited to allow a structure to be determined. However, it was concluded [16] that the parameters determined were consistent with the BF_3 being bound to a nitrogen in each heterocyclic with a B–N bond distance of roughly 1.61 Å.

In the investigation described in this article it was

assumed from the outset that the interaction between BF_3 and the nitrogen heteroatom predominates to such an extent that, to a first order of approximation, other interactions could be neglected. It was then reasoned that the number of BF_3 molecules, which could then be attached to a homogeneous cluster of a given size would depend on its structure and would, moreover, indicate the number of “unoccupied” nitrogen atoms available for bonding with BF_3 in the cluster. In this respect there are intuitively two fundamentally different types of structural configurations of heterocyclic molecules in homoclusters.

The first is one in which the main interaction takes place between the nitrogen atom and some other part of a neighboring molecule, for example, the π system of the ring or a hydrogen atom attached to the ring. In this case, a structure with a chainlike character would be formed and homoclusters of all sizes would only have one site available where strong bonding could occur (i.e. at the unoccupied nitrogen). The second is one in which an interaction between, for example, the π systems of adjacent rings predominates and a ring stacking (π stacking) results. In this case, the cluster has a number of equivalent complexation sites. Thus, by determining the number of BF_3 molecules that strongly attached themselves to a cluster, it would seem possible that we would be able to differentiate between structures of these two types.

The experimental results we obtained were, however, considerably more complicated than those anticipated. Although they do not provide unequivocal structural information over homoclusters, when combined with *ab initio* calculations, they do give insight into some of the properties of these clusters and also into those of the strongly bound donor–acceptor complexes.

The complexes we investigated were those formed by the reaction of the Lewis acids, BF_3 , BCl_3 , and $\text{B}(\text{OH})_3$ and the “classical” acids, HCl and HF , with clusters of several heterocyclic compounds.

The technique employed in this work was multiphoton ionization (MPI) of the clusters formed in an unskimmed, free-expansion jet. The ionized particles were then deflected into a linear time-of-flight mass spectrometer. Normally one would hope to gain some

information on the cluster involved by measuring spectroscopic band shifts as a function of cluster size or composition. However, under the conditions used, all the clusters studied displayed no resolvable spectral features at all. Consequently, the only data obtained from our measurements were those available from the mass spectra.

One point that may seem obvious, but that we wish to stress here, is that the *only* particles that appear in a mass spectrum are those for which the cation is sufficiently stable to survive the ionization process and actually arrive at the detector of the mass spectrometer (i.e. only particles with stable cations are registered). Thus, the nonappearance of certain mass signals may simply result because the cations of the particular species are unstable and not necessarily have any bearing on the concentration of that species present before ionization. As will be discussed in more detail later, although the 1:1 Py-BF_3 complex is certainly very stable, we arrive at the somewhat surprising conclusion that the cation of this complex is unstable and consequently not detectable in our experiments.

2. Experimental

The apparatus used to carry out MPI was the same as that used for spectroscopic studies of molecular complexes in this laboratory in the past [17,18]. In the present case, because none of the clusters investigated displayed resolvable spectral features, the output of the ionizing laser was kept fixed at a wavelength that produced the best signals over a wide mass range. The time-of-flight spectrometer consisted of a single vacuum chamber (~ 50 L volume) with the 50-cm-long drift tube aligned 90° the axis of the free expansion jet. The chamber and the drift tube were connected over an opening 5 mm in diameter. Pressures in the region of 10^{-4} mbar were maintained in the main chamber using a 1200 L/s diffusion pump, whereas the mass spectrometer was kept at 10^{-6} – 10^{-7} mbar with the aid of a 150 L/s turbomolecular pump.

Tunable ultraviolet radiation in the 240 nm region was produced by pumping a Lumonics HD-500 dye

laser with a XeCl excimer laser (Questek 3500) and then doubling the output in a BBO crystal (Lumonics HT1000). Pulse energies up to 10 mJ with pulse lengths of the order of 5 ns and a nominal line width of approximately 0.08 cm^{-1} were produced. In order to minimize photofragmentation, only a small fraction of the available pulse energy was focused into the vacuum chamber.

Frequency calibration of all the spectra reported in this paper was carried out using a Burleigh WA 4500 wavemeter. The ion signal was displayed on a digital oscilloscope (Tektronix TDS 320) and mass selected spectra were obtained by digitally recording the output of a box-car integrator (Stanford Research).

3. Cluster production and measurement

Homoclusters of the various heterocyclic compounds were produced by the usual expansion techniques. Argon saturated with the vapor pressure of, for example, pyridine at 50°C , was admitted at a stagnation pressure of 2 bar into the vacuum chamber through a pulsed nozzle (General Valve) with a 0.5 mm orifice. The resulting mass spectrum with the output of laser system kept fixed at 240 nm is shown in Fig. 1. As can be seen, after optimization of conditions, clusters with $n \leq 15$ were detected.

Under normal circumstances the donor–acceptor complexes studied here are all low vapor pressure solids; thus, in order to produce mixed clusters in the gas phase, the two components were brought together in the initial stage of the expansion process. The dual pulsed-valve nozzle used in this work is shown schematically in Fig. 2. It consisted of two pulsed valves (General Valve) mounted close together. The output of each valve was then passed along a stainless steel tube with an inner diameter of 0.2 mm and a total length of a 24 mm. The ends of the tubes were cemented into a Al_2O_3 ceramic tube, which formed an expansion mixing chamber 1 mm in diameter and 5 mm long.

The use of small diameter tubes as expansion nozzles changes the form of the gas expansion pulse compared with that produced by a pinhole orifice.

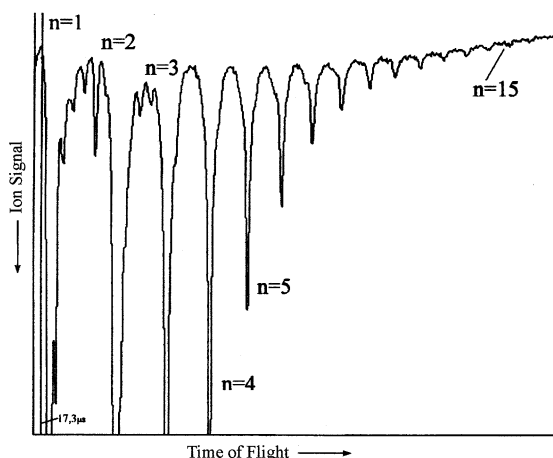


Fig. 1. Homogeneous clusters of pyridine, $(\text{Py})_n$, observed with $n \leq 16$ and produced using a pin-hole nozzle with approximately 80 mbar pyridine vapor in argon at a total stagnation pressure of 2 bar. Using the nozzle shown in Fig. 2 under similar conditions, signals with $n \leq 6$ were observed. Nonresonant, two-photon, ionization at 240 nm.

However, as past experience has shown [19], even with a tube of this type, several centimeters in length, expansion cooling could still be produced. The main effect of the introduction of the narrow tube is that the

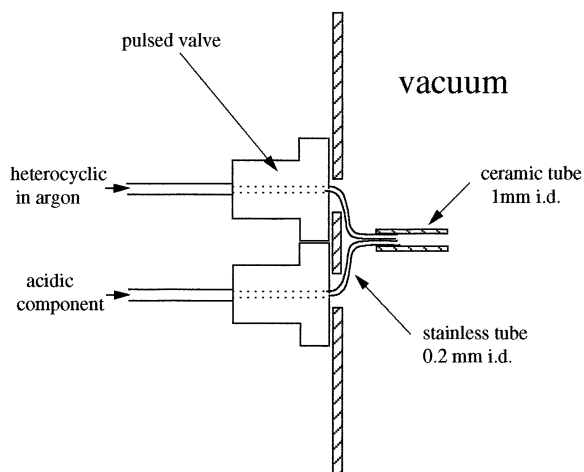


Fig. 2. The dual-pulsed nozzle used in this work. The output of two pulsed valves (General Valve) passed along two stainless steel tubes with inside diameter (i.d.) of 0.2 mm into a small mixing chamber. This consisted of a ceramic tube 1 mm i.d. and an effective length of 5 mm. No mixed clusters were formed without the mixing chamber.

gas pulse tends to be elongated and “smoothed” by the passage through the tube, so that a longer pulse at lower expansion pressure emerges from its end.

3.1. BF_3 mixed clusters

Argon containing the vapor of the heterocyclic under consideration was introduced at a stagnation pressure of 2 bar through one valve, and a 50% mixture of BF_3 in argon at a maximum pressure of 4 bar was admitted through the second valve. Observations were carried out using the following procedure. With the BF_3 valve closed, the parameters of the first valve (pulse length, delay time) were first adjusted to produce good signals for the homoclusters. Because the cooling produced by the tube nozzle was not as effective as with a pin-hole nozzle, in the case of pyridine, clusters $n \leq 6$ could be observed. The voltage pulse on the BF_3 valve was slowly increased until the first signals from mixed clusters were observed. After adjustment of the delay time, the quantity of BF_3 admitted into the mixing chamber could be effectively controlled via the length of the gas pulse put into the BF_3 line.

The mass signals observed with pyridine and a small amount of BF_3 are shown in Fig. 3(a), and the result of increasing the quantity of BF_3 admitted into the chamber is shown in Fig. 3(b). These mass spectra for pyridine with BF_3 are representative of the behavior of all the other heterocyclic compounds for which mixed-clusters were observed and the key points of the observations are tabulated here:

1. At low BF_3 concentrations, mixed clusters containing one BF_3 molecule predominated. These are indicated as $2 + \text{BF}_3$, $3 + \text{BF}_3$, and $4 + \text{BF}_3$ in Fig. 3(a). No signal was observed at the mass number of the 1:1 complex ($1 + \text{BF}_3$ in the above nomenclature).
2. Increasing the amount of BF_3 introduced into the mixing jet caused (1) the signals of the cluster containing one BF_3 molecule to increase, (2) the signals for the homoclusters to decrease, and (3) signals from clusters containing more than one BF_3 to appear [Fig. 3(b)].

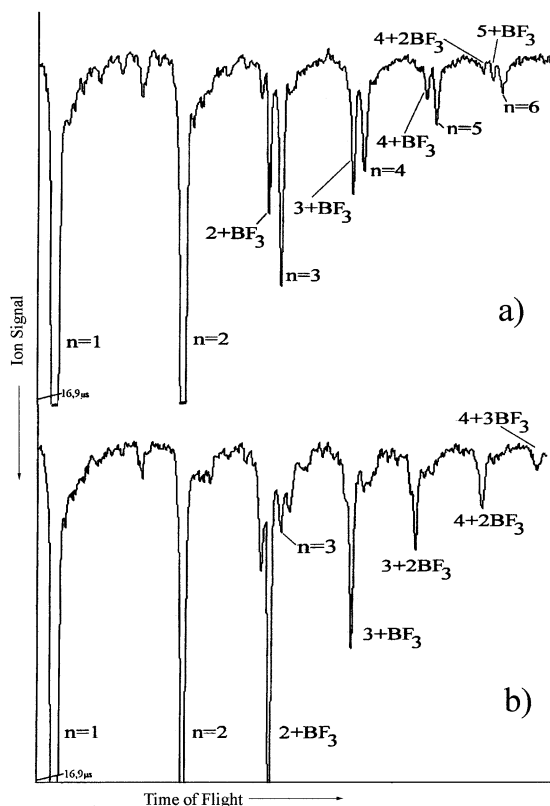


Fig. 3. The mixed-clusters formed between pyridine and BF_3 . (a) At low concentrations of BF_3 , clusters containing *only one* BF_3 predominate. (b) As more BF_3 is introduced, the signal strength of the mixed clusters increases at the expense of that of the homoclusters and signals from clusters containing more than one BF_3 molecule appear. By varying the open time of the BF_3 valve, a smooth change from a situation where no mixed clusters were observed, through the conditions shown in (a) to those shown in (b) was observable in real time. This allowed the determination of the interdependency of the strength of the homo- and the mixed cluster signal strengths to be repeatedly verified. Identical observations were made with 3-picoline. Nonresonant, two-photon, ionization at 240 nm.

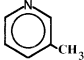
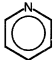

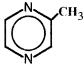
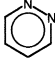
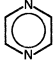
3. By continuous variation of the BF_3 gas pulse, it was possible to observe, in real time, a smooth change in the mass spectra from the initial situation where the first mixed-cluster peaks appeared, to the situation beyond that shown in Fig. 3(b) with a large quantity of BF_3 , where the only peaks originating from homoclusters were those with $n = 1$ and $n = 2$.

4. Under no circumstances were mass peaks of mixed cluster $(\text{Het})_n:(\text{BF}_3)_m$ with $n = m$ (i.e. 1:1, 2:2, and 3:3 complexes) observed. This situation remained unchanged, even when high laser powers were used (i.e. signals at the relevant mass numbers could not be produced by fragmentation of higher clusters).

The experimental arrangement used here makes it very difficult to quantify the relative concentrations of pyridine vapor and BF_3 gas in the mixing volume. However, in the initial measurements a 20% mixture of BF_3 in argon was used and under these circumstances only mixed-clusters containing *one* BF_3 molecule were observed. The results shown in Fig. 3(b) were achieved only after the concentration of BF_3 had been increased to 50%. This would seem to indicate that an extremely large excess of BF_3 was required to produce mixed clusters containing more than one BF_3 molecule.

The results of similar measurements using BF_3 with the heterocyclics, 3-picoline, 4-picoline, pyrazine, 2-methyl pyrazine, and pyridazine, are summarized in Table 1. The substances are arranged in the order of decreasing tendency to form homoclusters. For this purpose, factors such as the relative intensities of the mass peak of the monomer and that of the dimer and the maximum size of the clusters, as observed in our experiments, were used as a rough scaling factor. In view of the differing physical properties of the individual compounds it is unlikely that the detail of this arrangement is reliable. For example, although the temperature of the sample holder was adjusted in accordance with vapor pressure data, the partial pressure of the heterocyclic in the argon carrier gas could have varied considerably. What was very clear, however, was that the highest propensity for clustering was displayed by 3-picoline, closely followed by pyridine and 4-picoline. The other three compounds, each of which contain two heteroatoms, showed considerably less tendency to form homoclusters and thus their position in the lower half of Table 1 is certainly correct. Their positions relative to each other in Table 1 is, however, somewhat arbitrary.

Table 1
Cluster formation of six heterocyclic compounds with themselves and boron trifluoride

| Compound | pK_a^a | Maximum n^b | Mixed clusters |
|---|-----------------|----------------------|--|
|  3-Picoline | 5.68 | 8 | $n = 2$ to $5 + 1\text{BF}_3$ $n = 3$ to $4 + 2\text{BF}_3$ |
|  Pyridine | 5.25 | 6 (15 ^c) | $n = 2$ to $5 + 1\text{BF}_3$ $n = 3$ to $4 + 2\text{BF}_3$ $n = 4 + 3\text{BF}_3$ |
|  4-Picoline | 6.02 | 5 | $n = 2 + 1\text{BF}_3$ |
|  2-methyl pyrazine | 1.45 | 5 | $n = 2$ to $3 + 1\text{BF}_3$ |
|  Pyridazine | 2.25 | 5 | No signal |
|  Pyrazine | 0.65 | 5 | No signal |

^a Value refers to the protonated species.

^b Number of heterocyclic molecules in the homocluster.

^c Formed in single nozzle.

The formation of mixed clusters followed a similar pattern to that observed for the homoclusters. Pyridine and 3-picoline showed very similar properties and 4-picoline displayed a definitely reduced tendency to form mixed clusters. The most surprising result was that we observed no mixed clusters at all for both pyrazine and pyridazine (Table 1). We had anticipated an increase in the formation of mixed-clusters with these compounds. The only compound containing two heteroatoms for which mixed clusters were observed was 2-methyl pyrazine.

3.2. Mixed clusters with other acids

For comparison purposes, it was considered desirable to obtain data of mixed clusters with other Lewis acids. The obvious step was to investigate complexes formed with BCl_3 . The measurements with BCl_3 proved to be much more difficult than those with BF_3 . The main problem was produced by the sensitivity of

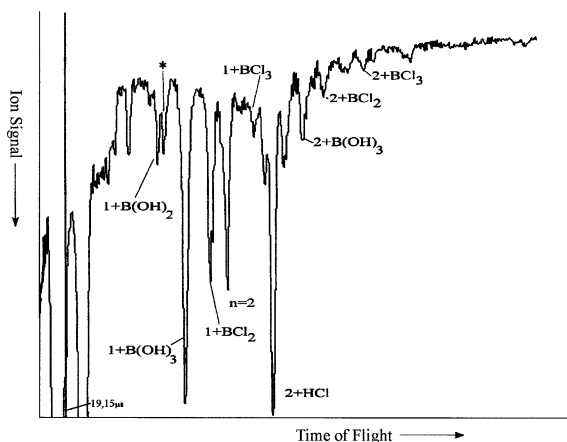


Fig. 4. The signals observed with 3-picoline (3-Pic) and BCl_3 . The mass spectrum at first displayed only signals from the mixed clusters of 3-picoline with the hydrolysis products of BCl_3 , B(OH)_3 , and HCl . The first signals from clusters containing BCl_3 were only observed after large quantities of the gas were passed into the system. Even under these conditions, the strongest signals arose from the 1:1 complex of 3-picoline with boric acid [B(OH)_3] and HCl . However, a strong signal for the 1:1 complex with the photolysis product of BCl_3 , BCl_2 , was observed and also a weak signal for the (3-Pic): BCl_3 1:1 complex.

BCl_3 to traces of water in the apparatus, reacting to form boric acid [B(OH)_3] and HCl . Indeed at first, only mixed complexes with these reaction products were observed. However, because boric acid is an acid, and HCl is the archetype acid, the production of mixed clusters with these species is also relevant to the present discussion.

Weak signals of the 1:1 complex of 3-picoline with BCl_3 were observed only after purging the apparatus with large quantities of BCl_3 . At no stage were we able to eliminate the signals from clusters formed with the hydrolysis products. The mass spectrum obtained with 3-picoline and BCl_3 is shown in Fig. 4. Only relatively weak signals were observed with mixed clusters formed between 3-picoline and BCl_3 . Much stronger mixed-cluster signals were observed for the hydrolysis products, B(OH)_3 and HCl . Even the fragmentation product, BCl_2 , produced stronger signals than BCl_3 . Another unusual aspect of this spectrum is the strong signal for the 2:1 mixed cluster consisting of a picoline dimer with one HCl molecule ($2 + \text{HCl}$ in Fig. 4), whereas the signal from the 1:1

Table 2

Mixed clusters observed with BCl_3 , HF , and HCl

3-picoline with BCl_3 and the hydrolysis products of BCl_3 (Fig. 4)

$n = 1$: $1 + \text{BCl}_3$, $1 + \text{BCl}_2$, $1 + \text{B(OH)}_3$, $1 + \text{B(OH)}_2$

$n = 2$: $2 + \text{BCl}_3$, $2 + \text{BCl}_2$, $2 + \text{B(OH)}_3$

Pyridine with 3% HF in helium (Fig. 5)

$n = 1$: no signal

$n = 2$: $2 + \text{HF}$ ($2 + \text{HCl}$)^a

$n = 3$: $3 + \text{HF}$ ($3 + \text{HCl}$)^a

Pyridine with 5% HCl in helium (Fig. 6)

$n = 1$: no signal

$n = 2$: $2 + \text{HCl}$, $2 + 2\text{HCl}$

$n = 3$: $3 + \text{HCl}$, $3 + 2\text{HCl}$, $3 + 3 \text{HCl}$

$n = 4$: $4 + \text{HCl}$, $4 + 2\text{HCl}$

^a HCl produced by reaction with apparatus.

complex is questionable (marked with an asterisk in Fig. 4). In the case of boric acid, however, a strong signal was observed for the 1:1 complex. These results are summarized in Table 2.

Having observed the formation of mixed clusters containing HCl by accident in the above work, it was decided to investigate clusters of this type a little more thoroughly. Two different gas mixtures were used as sources for HF and HCl . The first contained 3% HF in helium, the second 5% HCl in helium. The results of introducing considerable concentrations of these gas mixtures into the expansion of pyridine in helium is shown in Figs. 5 and 6, respectively, and the resulting mixed clusters observed are listed in Table 2.

At first it proved difficult to produce clusters containing HF . This is presumably caused by the concentration of HF actually reaching the output of the nozzle being kept small via reaction with the materials of the apparatus. This is illustrated by the appearance of clusters containing HCl , whereas the gas mixture used contained none. The HCl was presumably generated by reaction of HF with the walls of the apparatus, which had previously been used with BCl_3 . After a period of passivation, we succeeded in producing the results shown in Fig. 5. As can be seen (Table 2), only clusters containing one HF molecule were observed, but the 1:1 complex was not present.

No problems were encountered with the production of mixed-clusters with the HCl gas mixture. As can be seen in Fig. 6 and Table 2, here again the 1:1

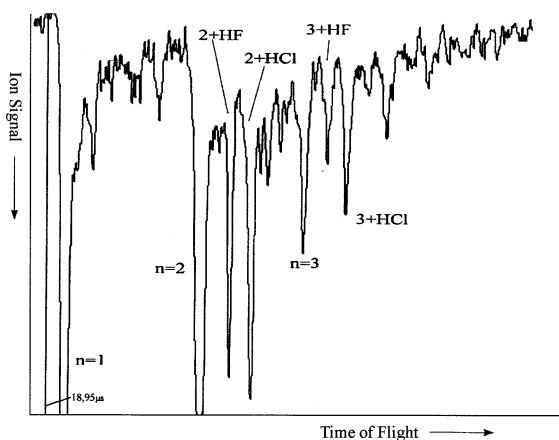


Fig. 5. The mass signals observed with pyridine and 3% HF in helium. The HCl present was produced by reaction of HF by contamination of the apparatus caused by the use of BCl_3 . Although clusters with $n = 2$ and $n = 3$ with one HF molecule were observed ($2+\text{HF}$ and $3+\text{HF}$ above), the 1:1 complex was not observed.

complex was missing, but a weak signal that was assigned as the 2:2 complex ($2+2\text{HCl}$ in Fig. 6) was observed.

4. Discussion

4.1. MPI process

The ionization potential (IP) of pyridine is approximately $78,235 \text{ cm}^{-1}$ (9.7 eV [14]). The $\pi-\pi^*$ transition frequency has been remeasured in this laboratory to be $38,617 \text{ cm}^{-1}$ (259.026 nm). This value lies between those previously reported [20,21]. Thus, when performing resonance enhanced MPI (REMPI) on pyridine using this transition, a second photon falls short of the IP by approximately 1000 cm^{-1} . Consequently, the process involved in the REMPI situation is a (1 + 1 + 1) process involving Rydberg levels below the IP and this three photon process produces an excess energy of roughly $37,000 \text{ cm}^{-1}$. For efficient cluster detection, a minimum of excess energy should be deposited in the cation. For this reason it was considered more advantageous to use a nonreso-

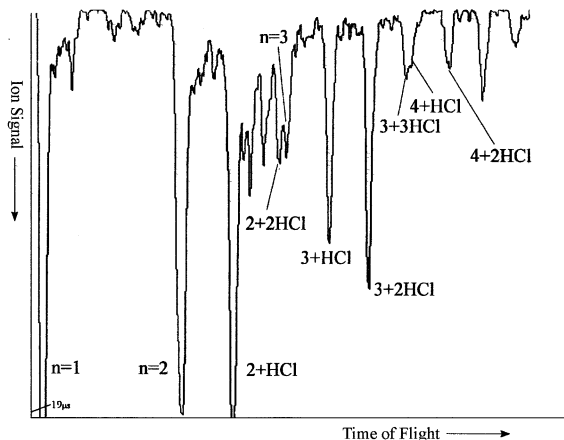


Fig. 6. The mass spectrum observed with pyridine and 5% HCl in helium. Although the signals from mixed clusters involving one HCl molecule predominate, in this case two signals from complexes with $n = m$, $2+2\text{HCl}$ and $3+3\text{HCl}$, are present. The 1:1 complex, $\text{Py}:\text{HCl}$, was, however, not observed.

nant ionization scheme. The choice of the wavelengths used in this work was influenced by the above consideration and practical factors determined by the laser system. The frequency doubler used allowed wavelengths down to 230 nm to be produced, but in terms of output, the best region was 240 nm, which corresponds to a photon energy of about $41,670 \text{ cm}^{-1}$. Although the IP of the clusters has not been measured, they are presumably not very different from pyridine itself and pyridine and its homoclusters were efficiently ionized at this wavelength via a nonresonant, two-photon process. Thus, by using 240 nm, the clusters were probably produced with considerably less excess energy than if 259 nm was employed. In practice, wavelength considerations seemed to have only minor influence on the mass spectra observed (i.e. the clusters survive the ionization process very well). This requires that at least the cation of homoclusters should be reasonably stable. As the ab initio calculations (discussed later) show, although the neutral pyridine dimer appears to be only weakly bound, its cation is considerably more stable. These points are significant when it comes to the consideration of the mechanism by which the mixed clusters are formed.

4.2. Photoionization of mixed clusters and the missing 1:1 complexes

In the case of the mixed clusters with BF_3 the IP is probably considerably higher than that of the heterocyclic itself. In the case of the 1:1 Py- BF_3 complex, the IP has been determined [14] to be 10.87 eV ($\sim 87,670 \text{ cm}^{-1}$). In this case, the shortest wavelength that our laser system could produce (230 nm) was barely enough for a two-photon process to produce ionization.

Because BF_3 is very electronegative (IP = 15.95 eV [14]), the ionization potential of all mixed clusters with $n = m$ is probably considerably higher than that of the homoclusters. It would also seem reasonable that clusters containing fewer BF_3 molecules have a lower IP.

At first this was considered to be the reason for the nonappearance of the 1:1 complex and all other $n = m$ complexes (i.e. these were simply not photoionized and therefore did not appear in the mass spectrum). However, it now seems almost certain that the primary reason for their nonappearance is related to an unstable cation rather than to difficulties with achieving photoionization.

The experimental data that led us to this conclusion are as follows:

1. Experiments with the mixed clusters carried out with high laser powers failed to produce a signal for the 1:1 complex. The power levels available from our laser system were certainly sufficient to produce at least some ionization by multiphoton processes if this was the problem. This was demonstrated to our satisfaction by the observation of the mass spectrum of BF_3 and its fragments. In this case, a four-photon process was required for ionization.
2. Although in the mass spectra like those of Fig. 3(a) and (b), many mass peaks corresponding to mixed clusters of various values of n and m were observed, under no circumstances was a mass peak for a complex with $n = m$ observed. If the cation of the 1:1 complex were stable (as the neutral species certainly is), by varying experimental con-

Table 3

Complexes formed between pyridine and acidic molecules and the cations detected

| Before ionization | After ionization | |
|--|---|---------------|
| Neutral | Ion | Neutral |
| Py: BF_3 | Py ⁺ | BF_3 |
| (Py) _n :(BF_3) _n ^a | (Py) _n (BF_3) _(n-1) ⁺ | BF_3 |
| Py:HF | Py ⁺ | HF |
| Py:HCl | Py ⁺ | HCl |
| (Py) ₂ :(HCl) ₂ | (Py) ₂ :(HCl) ₂ ⁺ | |
| Py: BCl_3 | Py: BCl_2^+ | Cl |
| | Py: BCl_3^+ | |
| Py:B(OH) ₃ | Py:B(OH) ₃ ⁺ | |

^a If formed; see text.

ditions one would expect at some stage to observe a signal from at least a fragment from higher clusters.

With hindsight, this situation can be easily rationalized. On ionization, the 1:1 cluster fragments into a pyridine cation and a neutral BF_3 molecule (i.e. the electronegativity difference between the two components of the complex leads to BF_3 retaining all its electrons and not forming a stable complex ion with pyridine).

This explanation is supported by the results with the other acids. The observations made for the complexes of the various acidic species investigated in this work with pyridine are summarized in Table 3.

HF also failed to produce a signal for the 1:1 complex or higher clusters with $n = m$ (Fig. 5). HCl, by contrast, appears to be an intermediate case, although no clear signal for the 1:1 complex was observed, a weak signal for the 2:2 complex appears to be present (Fig. 6). In the cases of BCl_3 and B(OH)_3 , which are considerably less electronegative than BF_3 , signals were observed for the 1:1 complex for both these species (Fig. 4).

A question that must be addressed to rationalize these observations is how can the interaction involved in the formation of the complexes investigated here be best described?

In solution, this could certainly be described as an acid-base reaction. There have been a number of reports on the determination of the values for acidity

and basicity in the gas phase for various substances and these quantities have been compared with the established values determined in solution [13,22]. Clearly, because we are dealing with Lewis acids like BF_3 , a system defining the acceptance or rejection of H^+ as the basis for a scale of basicity or acidity [13] is not applicable.

The approach of Lewis [23] in which this type of interaction is expressed in terms of electron donor and electron acceptor, is more suitable, but is not without its problems in the present discussion. It has been shown, for example, from x-ray crystallography data [24,25], that the B–N bond length in the pyridine complex with BCl_3 is shorter than that in the BF_3 complex. On the basis of data of this type, BCl_3 is classified as a stronger Lewis acid than BF_3 and $\text{B}(\text{OH})_3$ is very much weaker than both. In terms of observing a signal for the 1:1 complex, a positive result was achieved for the strongest and weakest bound complex, but not for the intermediate case. There is also the problem of where do HF and HCl now lie on this scale?

The problem of classification in relation to our experiments arises from the fact that not only the strength of the bonding in the neutral complex is important, but also the stability of the cation of the complex.

The behavior of the complexes and their cations in these experiments are better classified along the lines of the electronegativity of the acids concerned. Chemical intuition then groups BF_3 with HF and BCl_3 with HCl. As can be seen from the data presented in Table 3, this classification correlates quite well with our observations.

4.3. Complexes with $n = m$ with $n > 1$

BF_3 complexes with $n = m$ with $n > 1$ were also not observed, and here the situation is more complicated. One possibility is that complexes with the equal numbers of heterocyclic molecules and BF_3 molecules are formed and are stable, but on ionization, the complex loses a neutral BF_3 molecule and appears as the cation of $(\text{Het})_n(\text{BF}_3)_{n-1}$. The other possibility is, that because of the structure of the homo cluster, the

number of sites of high electron density available for forming the complex (i.e. unoccupied nitrogen atoms) is less than “ n ,” and the complex was never formed.

The characteristics described in Table 3 would seem to be generally applicable to the other heterocyclics considered in this paper, but detailed investigation was only carried out on pyridine and 3-picoline.

4.4. The propensity for the formation of homoclusters

As already mentioned, measurements have been carried out to determine the acidity and basicity of various compounds in the gas phase [13,22]. These include extensive measurements on substituted pyridines [22]. Unfortunately, the experimental values reported do not include those for all the heterocyclics investigated here. In general, a near linear relationship was determined between the gas phase proton affinity and basicity in aqueous solution. Consequently, for our purposes we feel justified in considering the conventional values of acidity/basicity such as pK_a in this discussion.

The pK_a values associated with the heterocyclics used in this work are included in Table 1. Although the detailed arrangement is not identical, the group with high basicity (3- and 4-picoline and pyridine, pK_a values of 5.25–6.02) showed the highest propensity for the formation of both homo- and mixed clusters; those with low basicity (pyridazine, 2-methyl-pyrazine, and pyrazine, pK_a values of 0.65–2.24) were considerably less efficient at forming both cluster types.

This correlation would seem to confirm that basicity is a key factor in influencing the formation of both homo- and mixed clusters. Although this is immediately acceptable when considering the formation of complexes with acidic species, the role of basicity in the formation of homoclusters would not seem to be so obvious. The explanation would seem to lie with the factors that determine the property termed “basicity.” If this is understood in terms of proton affinity, this is in effect a way of defining the extent to which a molecule possesses regions of high electron density.

In this sense, molecules with high Lewis basicity are probably more easily polarizable, and these are perhaps the main factors affecting the formation of homoclusters.

One result that seems to deviate slightly from this general rationalization, is that we observed no signal for a mixed-cluster with BF_3 and pyridazine, although these were observed with 2-methyl pyrazine, which is less basic than pyridazine (Table 1). This result may be because of experimental factors rather than really because mixed clusters were not formed by pyridazine.

4.5. Mechanism of mixed-cluster production

So far we have only considered the information yielded by the mass spectra observed under specific experimental conditions. The spectra observed indicate the end results of the cluster formation and ionization processes. Thus, it is clear that even if a particular complex is abundant in the jet before ionization, what is observed is critically dependent on the stability of the cation produced. Equally certain is that signals of low mass number can originate from fragmentation processes. This is particularly true, for example, of the $n = 1$ peak (pyridine itself) in Fig. 3(a) and 3(b). This signal originates partly from single pyridine molecules already present in the jet but also partly from photodissociation of higher clusters, for example, from the 1:1 Py- BF_3 complex. As discussed above, the elimination of a neutral BF_3 molecule from all the $n = m$ hetero-complexes on photoionization would result in contributions to the signals observed for the $m = (n - 1)$ complexes.

The question that has so far not been addressed directly, is how are the mixed-clusters formed in the free-expansion jet? At least two distinct processes could lead to their formation: (1) BF_3 molecules could attach themselves to homoclusters that had already formed or (2) large quantities of the strongly bound 1:1 Py- BF_3 complex could first form, followed by further clustering with further 1:1 Py- BF_3 complexes or with homoclusters of varying sizes.

The first mechanism closely approximates the original idea of gaining structural information over

homoclusters by observing their reaction with BF_3 . The second is a much more complex situation that would only yield information on the relative stabilities of various mixed clusters. Several experimental observations led us to believe that, under the conditions used here, the first mechanism predominates.

Although homoclusters are easily formed in a free-expansion gas jet, in order to observe signals from the mixed clusters, a postexpansion mixing chamber was required in these experiments. In our initial attempts to observe mixed clusters, two overlapping, parallel gas jets from two nozzles separated by 0.5 mm were used. Under these conditions, no signals from mixed clusters were detected. The first signals were observed only after addition of the short, ceramic, mixing chamber. This point will be discussed later in more detail in the section on ab initio calculations.

The basic requirement of any bond-forming process between two particles is that in order to achieve a stable condition, the new complex must relieve itself of, or at least redistribute, an amount of energy approximately equivalent to the dissociation energy of the bond being formed. Because the formation of homoclusters is seen to occur in a gas expansion, the relaxation processes available must be sufficient to allow this to happen. Because the homoclusters appear to be weakly bound, the energy required to be disposed of is correspondingly small. However, in the case of the mixed complexes, the binding energy involved is considerable, and it would appear that additional relaxation processes are required to allow bond formation. This correlates with the experimental observation that an additional mixing chamber was required to produce the mixed clusters. If the expansion process within this chamber is considered in detail, it may be reasonable to expect that in the initial stage of the expansion the formation of homoclusters would be favored, with the effects of the mixing chamber, which enable the formation of mixed clusters with BF_3 , occurring at a slightly later stage.

Another piece of experimental data also supports the hypothesis that the homoclusters are the first to be formed (i.e. mechanism 1 above). Fig. 3(a) and 3(b) show the mass spectra observed with low and high

concentrations of BF_3 , respectively. As mentioned earlier, in the actual experiments we were able to reproducibly observe the changes in relative signal strengths as a function of the quantity of BF_3 introduced into the expansion. The behavior observed was that the strength of the mixed clusters grew at the expense of signals of the homoclusters. For example, in Fig. 3(a), the $n = 3$ signal is much stronger than that of $(3 + \text{BF}_3)$, whereas in Fig. 3(b) the situation is reversed. The same is true of $n = 4$ and to a lesser extent $n = 2$. Although the signal for $n = 2$ has almost certainly a strong contribution from fragmentation, it also shows the same tendency as that for $n = 3$ and $n = 4$, indicating that the number of pyridine dimers is being depleted to form the $2 + \text{BF}_3$ complex.

The $n = 1$ (pyridine) signal is a less sensitive indicator of the mechanism involved, because it derives from a number of sources. However, in accordance with the mechanism proposed, this signal remains unchanged in the presence of varying amounts of BF_3 .

5. Ab initio calculations

In order to help clarify the situation, ab initio calculations using the program package Gaussian 94 [26] were carried out. The Hartree-Fock method is sufficient to describe donor-acceptor complexes formed between heterocyclic molecules and strong Lewis acids (e.g. Py-BF_3). The bonding in the pyridine dimer is, however, considerably weaker. Depending on the actual structure of the dimer being considered, the density functional method B3LYP and the second order Moller-Plesset perturbation theory (MP2) were applied in order to include the effects of electron correlation.

It was the aim of our calculations to determine the most stable structure of the complex concerned and to estimate its binding energy. An accurate calculation of the binding energies is beyond the scope of this work. In order to avoid excessive computational effort, vibrational corrections and the effects of basis set superposition were not taken into account.

In order to avoid effects arising from symmetry constraints, such as the location of saddle points rather than true minima, an asymmetric geometry was always chosen for the starting point of the structure optimization calculation. Nevertheless, in critical cases a force field calculation was carried out in order to check for imaginary frequencies, which indicate that convergence to a saddle point had occurred. In order to allow minor relaxations of the structure of the constituents of the complexes, all optimizations of the structures were carried out without applying any constraint to their geometry.

5.1. 1:1 Py-BF_3 and 1:1 Py-HF complexes

Basis set effects for donor-acceptor complexes of this type were first examined for the smallest prototype, the ammonia- BF_3 complex. Hartree-Fock calculations were carried out on this complex using different basis sets from STO-3G to 6-31+G*. The latter basis set accurately reproduced the rotational constants of this complex determined by Legon and Warner in their microwave investigation [1].

These preliminary investigations would seem to show that for the donor-acceptor complexes involving a B-N bond of interest in this work, the structural information produced by calculations using a 6-31+G* basis set were sufficiently accurate for our purposes. A preliminary search of a large number of possible structures was carried out using the cheaper STO-3G basis set.

5.2. 1:1 Py-BF_3 complex

Hartree-Fock calculations were carried out for the 1:1 Py-BF_3 complex with the STO-3G, 3-21+G, 6-31+G*, and the 6-311+G** basis sets. The B-N bond lengths, $r_{\text{B-N}}$, and estimated values of the donor-acceptor binding energy, $\Delta E(\text{Py-BF}_3)$, are listed in Table 4.

The heat of formation of the 1:1 Py-BF_3 complex in the reaction of gaseous pyridine and BF_3 to the *crystalline complex* was determined experimentally by Lappert and Smith [27] to be $\Delta H = -46 \pm 2$ kcal/mol. Although the binding energy calculated

Table 4
Calculated parameters of the 1:1 pyridine-BF₃ complex^a

| Basis set | <i>E</i> (Py) (Hartree) | <i>E</i> (BF ₃) (Hartree) | <i>E</i> (PyBF ₃) (Hartree) | ΔE (kcal/mol) | (B + C) (GHz) | <i>r</i> _{B-N} (Å) | μ (D) |
|-----------|----------------------------|--|--|--------------------------|------------------|--------------------------------|--------------|
| STO-3G | -243.6387 | -318.6619 | -562.3207 | -12.6 | 1.630 | 1.909 | 6.0 |
| 3-21G | -245.3120 | -321.4658 | -566.8493 | -44.9 | 1.776 | 1.644 | 8.9 |
| 6-31+G* | -246.7035 | -323.2089 | -569.9443 | -20.1 | 1.758 | 1.664 | 8.5 |
| 6-311+G** | -246.7533 | -323.2848 | -570.0699 | -19.6 | 1.761 | 1.664 | 8.5 |

^a Calculations carried out using a restricted Hartree-Fock Hamiltonian.

with the 3-21G basis set (Table 4) is almost identical to this experimental value, the values obtained with the 6-31+G* and the 6-311+G** basis sets are considerably smaller (≈ -20 kcal/mol; Table 4). Before any comparison can be made, it must be remembered, however, that our calculated values are in effect *gas phase values* and consequently the experimental value [27] must be corrected for the heat of sublimation of the complex into the gas phase. Unfortunately, no direct measurement of the required quantity appears to have been made, and consequently the heat of sublimation of the Py-BF₃ complex was estimated from the thermodynamic data of similar molecules.

The entropy of vaporization of toluene and nitrobenzene is tabulated as being $\Delta S_{\text{vap}}^0 = 24.2$ cal/(mol K) and the entropies of fusion for these and similar molecules lie in a range, $\Delta S_{\text{fus}}^0 = 10 \pm 1$ cal/(mol K) [28]. From these data, we estimate that the heat of sublimation of the 1:1 Py-BF₃ complex, which has a melting point of 45 ± 1 °C and a boiling point of 300 ± 5 °C [29], to be approximately $\Delta H_{\text{subl}}^0 \approx 17$ kcal/mol. This allows the condensed phase heat of formation [27] to be corrected to the required gas phase value, with the result $\Delta H_{\text{gas}} \approx -29$ kcal/mol. This is in good agreement with the $\Delta H = -25$ kcal/mol determined for the same reaction carried out in nitrobenzene as solvent [30]. Because the difference between energy and enthalpy of the gas phase reaction is expected to be small compared with ΔH_{gas} , these values can be approximately equated to the binding energy of the 1:1 Py-BF₃ complex.

Despite an older investigation that indicated an even higher value for the heat of formation of the complex [29], it would seem probable that the binding

energy is less than -30 kcal/mol. This conclusion is supported by the data shown in Table 4. Although the 3-21G basis set produces a result that accidentally coincides with the condensed phase heat of formation [27], it is clear from the above discussion that this value is too large. (This point was overlooked in an earlier theoretical work [14] using the 3-21+G basis set on the 1:1 Py-BF₃ complex.) Although the numerical values obtained may still be in considerable error, the more extensive basis sets, 6-31+G* and the 6-311+G**, produce a smaller value that would seem to be a move in the right direction and moreover seem to converge to a value of $\Delta E \approx -20$ kcal/mol.

These latter two basis sets also produce the most satisfactory results for a number of other parameters of the 1:1 Py-BF₃ complex.

The B-N bond length was determined to be 1.604 Å in an x-ray study of a crystalline sample [25]. All the calculations predict a longer bond in the gas phase and the better calculations converge to a B-N bond length of ≈ 1.66 Å (Table 4).

A mean value of the rotational constant ($B_0 + C_0$) ≈ 1.735 GHz was determined from a low resolution microwave study of the complex [16]. All three of the more accurate calculations (Table 4) produce slightly larger values. A precise value is not to be expected because Hartree-Fock calculations are known to underestimate bond lengths and the parameter calculated is ($B_e + C_e$) and not that determined in the experiment [16].

The results obtained confirm the statement made above in connection with calculations on the NH₃-BF₃ complex, that the 6-31+G* basis set seems to be a good compromise between accuracy and computational effort.

Table 5
Parameters^a calculated for the “chainlike” structures of the pyridine dimer

| | 1,2'-chain (a) | 1,3'-chain (a) | 1-4'-chain (a) | 1-4'-chain (b) | 1-4'-chain (c) |
|-----------------------|----------------|----------------|----------------|----------------|----------------|
| ΔE (kcal/mol) | -3.0 | -3.7 | -3.8 | -1.9 | -4.0 |
| $r_{\text{N-H}}$ (Å) | 2.006 | 1.983 | 1.984 | 2.516 | 2.355 |
| μ (D) | 2.6 | 2.1 | 5.5 | 5.6 | 5.9 |

^a Values obtained from (a) B3LYP/STO-3G, (b) B3LYP/6-31+G*, and (c) MP2/6-31+G* calculations.

The dipole moment of the 1:1 Py-BF₃ complex calculated with this basis set was $\mu = 8.5 \text{ D}^a$. The only experimental result available is $\mu = 6.90 \pm 0.05 \text{ D}$ [31,32] in a benzene solution. It is, of course, well known that dipole moments are notoriously difficult to calculate accurately.

5.3. The cation of the 1:1 Py-BF₃ complex

By using the 6-31+G* structure of the neutral 1:1 Py-BF₃ complex as starting point, an unrestricted Hartree-Fock calculation on the cation of this complex was carried out by using the same basis set. In this case, no energy minimum was located with B-N distances up to 5 Å. The cation of the complex dissociates into a pyridine cation and a neutral BF₃ molecule. By using the STO-3G basis set for a similar calculation, the dissociation was followed up to a distance of 20 Å. This calculation confirms the conclusion drawn from our experimental observations that although the neutral 1:1 Py-BF₃ complex is strongly bonded, on ionization it dissociates into a pyridine cation and a neutral BF₃ molecule.

5.4. The 1:1 Py-HF complex and its cation

Similar calculations were carried out on the 1:1 pyridine-HF complex, and once again the corresponding cation was found to be unstable. The most stable structure of the neutral complex appears to be, as one would anticipate, one in which the H atom of the HF molecule is bound to the nitrogen of pyridine. Structures in which the F atom interacts with the hydrogens on the pyridine ring were found to be energetically less favorable by approximately 5.6 kcal/mol. The structure of the most stable configuration of the

complex was calculated by using a 6-31+G* basis set to have a H-N bond length of 1.79 Å. As already mentioned, in line with our experimental observations, the cation of the complex appears to be unstable.

5.5. The pyridine dimer and its cation

Quantum chemical calculations on the benzene dimer [33,34] predicted a T-shaped structure and a parallel displaced structure. The former structure was confirmed by microwave spectroscopy [35]. In the case of the pyridine dimer we also considered chainlike structures. Compared with benzene, the number of possible structures is increased considerably by the number of different relative orientations of the N atoms in the two rings.

The bonding in pyridine dimer can arise from both electrostatic interactions, mainly because of dipole and quadrupole moments, and from dispersion energy. The latter contribution is not reproduced by density functional methods like the hybrid functional B3LPY [36], which was used here in order to include the effects of electron correlation at moderate cost [37]. Structures in which dispersion energy was expected to make significant contributions were therefore calculated with MP2 perturbation theory.

The search for minima using B3LYP was carried out with the STO-3G basis set on a large number of starting positions for the three basically different structures mentioned above. In this case, minima were only located for the chainlike structures involving bonding between the nitrogen atom of one ring and one of the hydrogen atoms of the other ring. The binding energies to each of the hydrogens in 2-, 3-, and 4-ring positions appear to be all of the order of

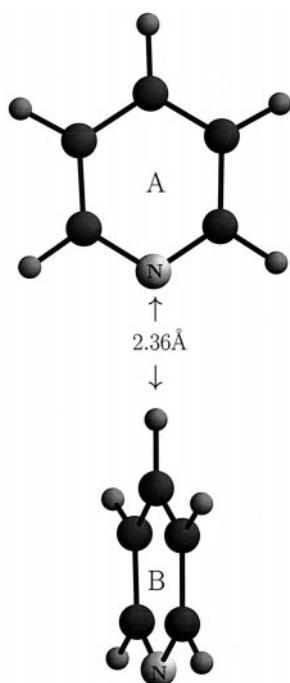


Fig. 7. The most stable chainlike structure of the pyridine dimer found by using a B3LYP/6–31+G* calculations. It is basically a linear configuration with the nitrogen of one ring attached to the hydrogen in 4-position on the other ring. The plane of the two rings, which are denoted as A and B, are perpendicular to each other to within a few degrees. MP2/6–31+G* calculations also produced a very similar structure, but indicated that it may be less stable than the parallel displaced structures of Fig. 8.

–3 kcal/mole and the results are shown in Table 5. The structures are referred to as 1,2'-, 1,3'-, and 1,4'-chains in Table 5 and, as expected, the dipole moment of the dimer increases from the 1,2'- to the 1,4'-chain. The pyridine ring with the free nitrogen atom is referred to as the “B-ring” in the following text, and the ring with its nitrogen atom bonded to the hydrogen atom of the other ring is referred to as the “A ring.” The bonding position in the B-ring is denoted by the primed number.

The most stable dimer structure found in the B3LYP/STO-3G survey was the 1,4'-chain and this structure (Fig. 7) was examined more accurately using B3LYP/6–31+G*. As can be seen from Table 5, this calculation predicted a somewhat weaker interaction between the two pyridine molecules, the binding

energy reducing to –1.9 kcal/mol and the N–H bond length increasing to 2.56 Å. In all calculations for the 1,4'-chain, the planes of the A and B rings were found to be approximately perpendicular to each other.

Starting from this structure for the neutral dimer, the structure of the cation was calculated by using the unrestricted B3LYP Hamiltonian and the 6–31+G* basis set (UB3LYP/6–31+G*). The structure of the cation is similar to that of the neutral dimer, but the binding energy increases. The results showed the dimer cation to be 16.1 kcal/mol more stable than a neutral pyridine molecule plus a pyridine cation and the N–H bond length reduced to 2.08 Å. The electric charge was found to be unequally distributed, with 0.64 e_0 on the B ring and 0.36 e_0 on the A ring.

In all dimer structures other than a linear chain, dispersion energy would be expected to play a more important role, and in these cases a search was carried out with MP2 perturbation theory with the 6–31+G* basis set.

The search for stable T-shaped structures were started from slightly asymmetric positions with the second pyridine lying nearly in a plane passing through the N and 4C atoms of the first pyridine molecule, or nearly perpendicular to this plane. Structures in which the nitrogen atom of the second pyridine pointed either toward, or away from, the ring of the other pyridine were considered. None of these positions resulted in a stable T-shaped structure, but one did result in a π -stacking type structure in which the centers of the two rings were displaced relative to the other [Fig. 8(b)]. We will refer to structures of this type as parallel, displaced dimer structures.

There is a large number of possible orientations of the two rings relative to one another in these parallel structures, but because of the large computational effort required for each, we have considered only the two extreme positions: the ones in which the molecular dipoles are parallel and antiparallel to each other (i.e. the nitrogen atoms of the heterocyclic rings point in the same or opposite directions). In order to be able to discuss dimer structures of this type we will introduce the parameters shown in Fig. 8(a): R is the distance between the two ring planes, and a parameter

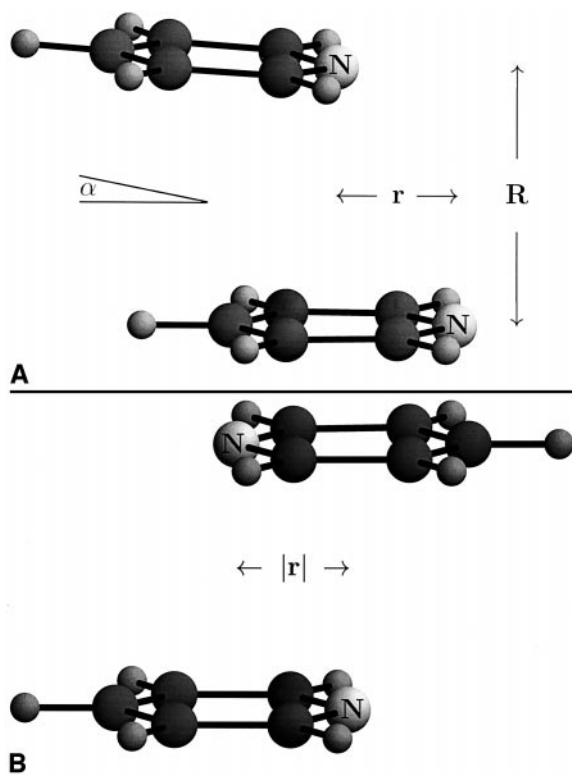


Fig. 8. Two “ π -stacking” type structures shown to be stable by MP2/6–31+G* calculations. In the resulting structures, the two rings are very close to being parallel to each other ($\alpha = 3.9^\circ$). Only the two extreme relative orientations of the rings with (a) the molecular dipoles parallel or (b) antiparallel to each other were considered. The values obtained for the two parameters R (the separation of the two ring planes) and r (the displacement of the two nitrogen atoms relative to one another) are given in Table 6. These structures appear to be more stable than that in Fig. 7 (see text).

r , where r is the projection of the separation of the two nitrogen atoms in the ring planes. When the two N atoms point in the same direction, r is considered to be positive; it is considered to be negative when the N atoms point in opposite directions [Fig. 8(b)].

The starting positions for the calculations were chosen to be those present in graphite ($R = 3.3 \text{ \AA}$, $r = \pm 1.5 \text{ \AA}$). The calculation with a positive value of r resulted in a minimum that was 5.3 kcal/mol more stable than two monomers. The angle α between the two ring planes was calculated to be 3.9° [Fig. 8(a)].

A parallel displaced structure with negative value of r resulted from a T-shaped starting structure and is

Table 6
Parameters^a calculated for the “parallel displaced” structures of the pyridine dimer

| Molecular dipoles directed | Parallel [Fig. 8(a)] | Antiparallel [Fig. 8(b)] |
|----------------------------|----------------------|--------------------------|
| ΔE (kcal/mol) | –5.3 | –6.1 |
| R (\AA) | 3.176 | 3.290 |
| r (\AA) | 1.700 | –1.347 |

^a For definition of parameters, see Fig. 8(a), values obtained from MP2/6–31+G* calculations.

the most stable dimer (–6.1 kcal/mol) obtained from MP2/6–31+G* calculations. In this case, the two rings are parallel to within less than 0.5° . The relevant data of the minima found in these calculations are listed in Table 6.

In order to compare the stability of the chainlike structures obtained with the B3LYP/6–31+G* with these latter structures, a MP2 calculation was carried out on the 1-4'-chain. This resulted in an increase in the binding energy to –4.0 kcal/mol compared with the B3LYP result of –1.9 kcal/mol. The two rings remained perpendicular to each other, but the N–H distance reduced to 2.36 \AA (Table 5). Because this MP2 calculation produced an increase in the stability of the 1-4'-chain, there appears to be no reason to suppose that similar results would not be obtained for the other chainlike structures considered here (Table 5). It would, therefore, seem reasonable to assume that the 1,2'-, 1,3'-, and 1,4'-chains, which were all predicted to be stable by the B3LYP calculations, are indeed stable isomers of the pyridine dimer.

The MP2/6–31+G* calculations showed that the three minima were located with stabilization energies varying from –4 to –6 kcal/mol, with the parallel, displaced structures appearing to be the most stable. However, it has been shown that in the case of benzene [34] the stability of this latter type of structure is overestimated in MP2 calculations, and it would seem, therefore, quite difficult to be sure which type of structure is really the most stable.

Thus in summary, our calculations have shown that three chainlike structures and at least two parallel, displaced structures appear to be stable for the pyridine dimer. The relative stability within the groups of

the same type of structure (i.e. those of Tables 5 and 6) would seem to be reliably predicted because these are mainly due to electrostatic differences. Although the parallel, displaced (π -stacking) structure with antiparallel dipole orientation [Fig. 8(b)] would seem to be most stable, the 1,4'-chain (Fig. 7) may in fact be of similar stability.

5.6. Complexes with the pyridine dimer

The cation of the 1:1 Py-BF₃ complex was found, in accordance with the experimental observations, to be unstable. Signals from the 2:1 (Py)₂-BF₃ complex were, however, detected (Fig. 3), and therefore structural information of this complex and its cation were of interest for comparison. It was not feasible to carry out MP2 calculations with our present computer facilities, and calculations were only carried out on the 1,4'-chain by using the small basis set, STO-3G. By using the data discussed above for the pyridine dimer, the complex was considered to be formed by a BF₃ molecule attaching itself to the nitrogen atom of the B ring of the 1,4'-chain structure of the pyridine dimer. The calculation resulted in a N-H bond length between the rings of 1.925 Å and a N-B bond length of 2.115 Å. The values for these two bond lengths in the pyridine dimer and the 1:1 Py-BF₃ complex, by using the same basis set, were $r_{\text{N-H}} = 1.984$ Å and $r_{\text{N-B}} = 1.909$ Å, respectively. This indicates that the bonding to the BF₃ molecule is weaker than in the 1:1 complex, but that the bonding between the rings is stronger than in the neutral pyridine dimer.

The 2:1 complex was found by a B3LYP/STO-3G calculation to be stable with respect to every possible dissociation pathway. It was 13.4 kcal/mol more stable than two pyridine molecules plus BF₃, 5.0 kcal/mol more stable than pyridine plus Py-BF₃, and 9.6 kcal/mol more stable than the 1,4'-pyridine dimer plus BF₃.

These values are of relevance to the above discussion on the mechanism of formation of the mixed-clusters. As can be seen, the formation of the 2:1 complex from the pyridine dimer plus BF₃ releases nearly twice the energy necessary for the dissociation of this complex into pyridine plus the 1:1 Py-BF₃

complex. As already discussed, the latter is not detectable in these experiments in any case. Consequently, for the 2:1 Py-BF₃ complex to be observable, a collision partner is required to accept >4.6 kcal/mol. This explains the necessity of the postexpansion mixing chamber for the production of the mixed clusters.

The cation of the 2:1 complex was found to be stable. Although the calculations, because of internal large amplitude motions, did not result in a well defined structure determination, the complex cation was shown to be more stable than any combination of dissociation products by at least 14 kcal/mol.

5.7. Structure of homoclusters with $n > 2$

Because we were unable to carry out accurate quantum-chemical calculations on clusters containing more than two heterocyclic molecules, the question to be discussed is, can any information be derived from the data available?

As the spectra show [Fig. 3(a)], at moderate concentrations of BF₃, mixed clusters involving *only one unit* of the acidic species appear to be preferentially formed. Unfortunately, this in itself does not necessarily prove that a single preferential bonding site (i.e. an unoccupied heteroatom) is present in the clusters.

As already explained, our observations in real time led us to the conclusion that in our experiments mixed-clusters were formed by the reaction of, for example, BF₃ with homoclusters that were already present. Under these circumstances, simply on the basis of the statistics of a collision occurring between a cluster and a BF₃ molecule, one would expect mixed clusters containing only one BF₃ molecule to be initially formed. It is very difficult to quantify the concentrations of pyridine vapor and BF₃ gas present in the mixing chamber of our dual nozzle. However, it would seem that, even under conditions used to produce the mass spectra of Fig. 3(a), such a large excess of BF₃ molecules was used that some factor in addition to simply collisional statistics would be required to cause preferential production of mixed clusters containing only one BF₃ molecule.

The ab initio calculations on the dimer came up with a structure with two equivalent heteroatoms, the parallel displaced structure with antiparallel dipole orientation [Fig. 8(B)], as the most stable. However, as already discussed, the other stable structures are not much less favorable and may indeed also be present. In the chainlike structures considered for the pyridine dimer (Fig. 7) it is obvious that one of heterocyclic atoms is, in the sense discussed earlier, an unoccupied, preferential bonding site. Even the other π -stacking type of structure discussed here [Fig. 8(A)], has a similar characteristic. So even if these latter structures are energetically less favored they may still represent a considerable portion of the dimers produced.

It is not clear to what extent the results with the dimer can be extrapolated to larger clusters. However, it seems quite possible that larger homoclusters with nonequivalent heteroatoms could be present. In such a case, one might expect to observe a preference for the formation of mixed-clusters involving *only one unit* of the acidic species.

As mentioned in the introduction, even when considering just a single pyridine, there are several potential bonding sites for BF_3 on the pyridine molecule, the electron lone pair on the nitrogen atom is simply the most energetically advantageous position. Thus, even if the pyridine homoclusters did possess a single preferential bonding site, at high concentrations of BF_3 it could well happen that further BF_3 molecules attach themselves to other sites on the cluster.

A further point that makes the situation even more difficult is that the addition of a single acidic molecule to a pyridine homocluster may in itself cause a considerable change in its properties. Thus, even in the event of clusters being present initially with several equivalent sites, once reaction has occurred, the probability of a second molecule attaching itself to the mixed-cluster would probably be reduced.

Although the experimental and theoretical information is inconclusive on this matter, it seems that the structures occurring in small clusters of heterocyclic compounds containing one nitrogen atom, such as pyridine and the picolines, may in fact possess a preferential bonding site or at least, they may have a

higher propensity for the formation of mixed clusters containing only a single acidic molecule.

6. Conclusions

It appears that the propensity for the formation of both homoclusters and mixed clusters is related to the basicity of the heterocyclic compound concerned.

The stability of the cation of the donor-acceptor complex formed is inversely related to the electron affinity of the acceptor (acidic) molecule. The ab initio calculations on the 1:1 pyridine- BF_3 complex confirm that the cation of 1:1 complexes with BF_3 and HF are unstable and dissociate on ionization into a heterocyclic cation and a neutral BF_3 (or HF) molecule. As the electron affinity of the acidic species reduces (e.g. BCl_3), the 1:1 complex appeared in the mass spectrum. The $n = m$ complexes with HCl appear to lie close to the borderline in this respect, because weak signals from these species were observed. In the case of the very weak (Lewis) acid, $\text{B}(\text{OH})_3$, the cation of the 1:1 complex is stable and a strong mass peak was observed (Fig. 4). The experimental and theoretical results indicate that on clustering, heterocyclic compounds containing one nitrogen atom may form structures with nonequivalent heterocyclic atoms.

Acknowledgements

This work is supported by the Deutsche Forschungsgemeinschaft and in part by the Fonds der Chemischen Industrie and the Eberhardt Stiftung.

References

- [1] R.D. Urban, M. Takami, J. Chem. Phys. 103 (1995) 9132.
- [2] T. Brupbacher, J. Makarewicz, A. Bauder, J. Chem. Phys. 108 (1998) 3932.
- [3] M. Gerhards, M. Schmitt, K. Kleinermanns, W. Stahl, J. Chem. Phys. 104 (1996) 967.
- [4] T. Weber, A.M. Smith, E. Riedle, H.J. Neusser, E.W. Schlag, Chem. Phys. Lett. 175 (1990) 79.

- [5] R.M. Helm, H.P. Vogel, H.J. Neusser, *J. Chem. Phys.* 108 (1998) 4496.
- [6] N.M. Lakin, G. Pietraperzia, M. Becucci, E. Castellucci, M. Coreno, A. Giardini-Guidoni, A. van der Avoird, *J. Chem. Phys.* 108 (1998) 1836.
- [7] J.R. Carny, F.C. Hagemeister, T.S. Zwier, *J. Chem. Phys.* 108 (1998) 3379.
- [8] S.K. Kim, S. Li, E.R. Bernstein, *J. Chem. Phys.* 95 (1991) 3119.
- [9] J. Wanna, J.A. Menapeace, E.R. Bernstein, *J. Chem. Phys.* 85 (1986) 1796.
- [10] L.L. Connell, T.C. Corcoran, P.W. Joireman, P.M. Felker, *Chem. Phys. Lett.* 166 (1990) 510.
- [11] T.A. Dang, R.J. Day, D.M. Hercules, *Anal. Chim. Acta* 158 (1984) 235.
- [12] R. Tembreull, C.H. Sin, H.M. Pang, D.M. Lubman, *Anal. Chem.* 57 (1985) 2911.
- [13] J-F. Gall, P-C. Maria, *Prog. Phys. Org. Chem.* 17 (1990) 159.
- [14] I.J. Hillier, M.A. Vincent, J.A. Connor, M.F. Guest, A.A. MacDowell, W. Von Niessen, *J. Chem. Soc. Faraday Trans. 2* 84 (1988) 409.
- [15] J.M. Yam, J.G. Zhao, *Int. J. Quant. Chem.* 27 (1985) 465.
- [16] W. Caminati, D. Damiani, *J. Mol. Struct.* 147 (1986) 389.
- [17] A.H. Bahnmaier, T. Engst, H. Jones, S.D. Colson, *Mol. Phys.* 82 (1994) 1203.
- [18] J-G. Jäckel, R. Schmid, H. Jones, T. Nakanaga, H. Takeo, *Chem. Phys.* 215 (1997) 291.
- [19] H. Birk, Doctorate thesis, Universität Ulm, D-89069 Ulm, Germany, 1992.
- [20] T. Kobayashi, S. Nagakura, *J. Electron Spectrosc. Relat. Phenom.* 4 (1974) 207.
- [21] I. Yamazaki, K. Sushida, H. Baba, *J. Chem. Phys.* 71 (1979) 381.
- [22] J-L.M. Abboud, J. Catalán, J. Elguero, R.W. Taft, *J. Org. Chem.* 53 (1988) 1137.
- [23] G.N. Lewis, *Valence and the Structure of Molecules*, The Chemical Catalogue, NY, 1923.
- [24] K. Töpel, K. Hensen, M. Trömel, *Acta Crystallogr. B* 37 (1981) 969.
- [25] K. Töpel, K. Hensen, J.W. Bats, *Acta Crystallogr. B* 40 (1984) 828.
- [26] M.J. Frisch, G.W. Trucks, H.B. Schlegel, P.M.W. Gill, B.G. Johnson, M. Robb, J.R. Cheeseman, T. Keith, G.A. Petersson, J.A. Montgomery, K. Raghavachari, M.A. Al-Laham, V.G. Zakrzewski, J.V. Ortiz, J.B. Foresman, J. Cioslowski, B.B. Stefanov, A. Nanayakkara, M. Challacombe, C.Y. Peng, P.Y. Ayala, W. Chen, M.W. Wong, J.L. Andres, E.S. Replogle, R. Gomperts, R.L. Martin, D.J. Fox, J.S. Binkley, D.J. Defrees, J. Baker, J.P. Stewart, M. Head-Gordon, C. Gonzalez, J.A. Pople, *Gaussian 94*, Revision E.1, Gaussian, Pittsburgh, PA, 1995.
- [27] M.F. Lappert, J.K. Smith, *J. Chem. Soc.* (1965) 7102.
- [28] R.C. Weast, M.J. Astle, W.H. Beyer, *CRC Handbook of Chemistry and Physics*, 66th ed., CRC Press, Boca Raton, FL, 1985.
- [29] P.A. van der Meulen, H.A. Heller, *J. Am. Chem. Soc.* 54 (1932) 4404.
- [30] H.C. Brown, R.H. Horowitz, *J. Am. Chem. Soc.* 77 (1955) 1730.
- [31] *Gmelin Handbuch der Anorganischen Chemie*, Ergänzungswerk zur 8. Auflage, Band 46, Borverbindungen Teil 15, Springer Verlag, Berlin, 1977.
- [32] C.M. Bax, A.R. Katritzky, L.E. Sutton, *J. Chem. Soc.* (1958) 1258.
- [33] P. Hobza, H.L. Selzle, E.W. Schlag, *J. Chem. Phys.* 93 (1990) 5893.
- [34] P. Hobza, H.L. Selzle, E.W. Schlag, *J. Chem. Phys.* 100 (1996) 18790.
- [35] E. Arunan, H.S. Gutowsky, *J. Chem. Phys.* 98 (1993) 4294.
- [36] P. Hobza, J. Sponer, T. Reschel, *J. Comp. Chem.* 16 (1995) 1315.
- [37] J.B. Foresman, E. Frisch, *Exploring Chemistry with Electronic Structure Methods*, 2nd ed., Pittsburgh, PA, 1996, and references therein.